



Published in final edited form as:

Cell Rep. 2016 March 22; 14(11): 2562–2575. doi:10.1016/j.celrep.2016.02.064.

The Innate Immune Receptor NLRX1 Functions as a Tumor Suppressor by Reducing Colon Tumorigenesis and Key Tumor-Promoting Signals

A. Alicia Koblansky^{1,8}, Agnieszka D. Truax^{1,8}, Rongrong Liu^{1,2,8}, Stephanie A. Montgomery^{1,3}, Shengli Ding⁴, Justin E. Wilson^{1,7}, W. June Brickey¹, Marcus Mühlbauer⁵, Rita-Marie T. McFadden¹, Peizhen Hu⁶, Zengshan Li⁶, Christian Jobin⁵, Pauline Kay Lund⁴, and Jenny P.-Y. Ting^{1,7,*}

¹The Lineberger Comprehensive Cancer Center, University of North Carolina, Chapel Hill, NC 27599-7295, USA

²Department of Microbiology, School of Basic Medicine, Fourth Military Medical University, Xi'an 710032, China

³Department of Pathology and Laboratory Medicine, University of North Carolina, Chapel Hill, NC 27599-7295, USA

⁴Department of Cell Biology and Physiology, University of North Carolina, Chapel Hill, NC 27599-7295, USA

⁵Department of Medicine, Division of Gastroenterology, University of Florida College of Medicine, Gainesville, FL 32611, USA

⁶Department of Pathology, Xijing Hospital, Fourth Military Medical University, Xi'an 710032, China

⁷Department of Genetics, University of North Carolina, Chapel Hill, NC 27599-7295, USA

SUMMARY

NOD-like receptor (NLR) proteins are intracellular innate immune sensors/receptors that regulate immunity. This work shows that NLRX1 serves as a tumor suppressor in colitis-associated cancer (CAC) and sporadic colon cancer by keeping key tumor promoting pathways in check. *Nlrp1*^{-/-} mice were highly susceptible to CAC, showing increases in key cancer-promoting pathways including nuclear factor κ B (NF- κ B), mitogen-activated protein kinase (MAPK), signal transducer and activator of transcription 3 (STAT3), and interleukin 6 (IL-6). The tumor-suppressive function

This is an open access article under the CC BY-NC-ND license (<http://creativecommons.org/licenses/by-nc-nd/4.0/>).

*Correspondence: jenny_ting@med.unc.edu.

⁸Co-first author

AUTHOR CONTRIBUTIONS

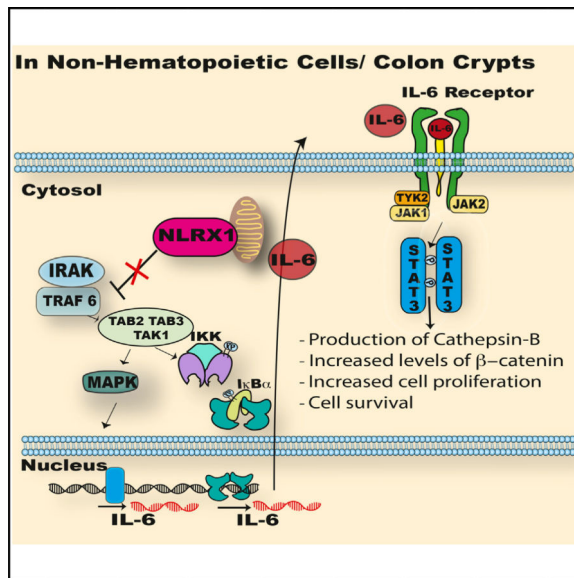
A.A.K., A.D.T., and J.P.-Y.T. designed experiments and wrote manuscript with insight from J.E.W., W.J.B., S.D., and P.K.L. A.A.K. performed immunoblots and analyses. A.D.T. and R.L. performed qPCR and analyses. A.A.K., A.D.T., W.J.B., J.E.W., and S.D. conducted CAC and *Apc*^{Min/+} mouse studies. R.L. and A.D.T. prepared human samples and analyzed datasets. S.D. performed FRI of intestinal tissues. P.H. and Z.L. obtained human samples. M.M., R.T.M., and C.J. performed mini-endoscopy. S.A.M. analyzed H&E slides and provided histopathological scoring. All contributing authors have agreed to submission of manuscript for publication.

SUPPLEMENTAL INFORMATION

Supplemental Information includes Supplemental Experimental Procedures and three figures and can be found with this article online at <http://dx.doi.org/10.1016/j.celrep.2016.02.064>.

of NLRX1 originated primarily from the non-hematopoietic compartment. This prompted an analysis of NLRX1 function in the *Apc^{min/+}* genetic model of sporadic gastrointestinal cancer. NLRX1 attenuated *Apc^{min/+}* colon tumorigenesis, cellular proliferation, NF- κ B, MAPK, STAT3 activation, and IL-6 levels. Application of anti-interleukin 6 receptor (IL6R) antibody therapy reduced tumor burden, increased survival, and reduced STAT3 activation in *Nlr1^{-/-}Apc^{min/+}* mice. As an important clinical correlate, human colon cancer samples expressed lower levels of *NLRX1* than healthy controls in multiple patient cohorts. These data implicate anti-IL6R as a potential personalized therapy for colon cancers with reduced NLRX1.

Graphical Abstract



INTRODUCTION

Members of the nucleotide binding domain and leucine-rich repeat-containing (NLR, also known as NOD-like receptor) family are evolutionarily conserved components of the immune system that are key mediators of immune defense and inflammation (Takeuchi and Akira, 2010). The major focus in the NLR field is on the inflammasome NLRs, which activate caspase-1 resulting in production of interleukin 1 β (IL-1 β) and interleukin 18 (IL-18). A subgroup of NLRs play an important role in the regulation of signaling pathways crucial for cell proliferation, survival, cellular differentiation, adhesion, migration, and metabolism, such as mitogen-activated protein kinases (MAPK) and nuclear factor κ B (NF- κ B) (Hayden and Ghosh, 2011; Sebolt-Leopold and Herrera, 2004; Wullaert et al., 2011). Aberrant activation of these pathways initiate and promote tumor development (Elinav et al., 2013); thus, it is important to determine if NLRs control these pathways during tumorigenesis and if these findings have translational relevance in human cancers.

Colorectal cancer (CRC) is the third most common cancer in both men and women and the second leading cause of cancer-related mortality in the United States with estimates of over 130,000 new cases diagnosed and 50,000 deaths in 2013 (Siegel et al., 2013). Recent studies

reported an increased frequency of colon cancer in adults younger than 50, with these patients more likely to show an advanced stage of the disease (Bailey et al., 2015). Over 90% of CRCs are adenocarcinomas, while rarer forms include neuroendocrine, squamous cell, spindle cell, and undifferentiated carcinomas (Fleming et al., 2012).

Colitis-associated colon cancer (CAC) accounts for 1% of CRC (Yashiro, 2014). The link between chronic inflammation and increased tumorigenesis has been well documented in inflammatory bowel diseases (IBD), including ulcerative colitis (UC), and Crohn's disease (CD) (Rogler, 2014; Terzi et al., 2010). IBD are associated with increased production of pro-inflammatory cytokines, which are associated with the activation of NF- κ B, signal transducer and activator of transcription 3 (STAT3), and mitogen-activated protein kinase (MAPK). Each of these pathways contributes to tumor progression in CRC (Ben-Neriah and Karin, 2011; Dhillon et al., 2007; O'Shea et al., 2013). NF- κ B regulation of CRC development occurs through the enhanced survival of pre-malignant epithelial cells and release of inflammatory cytokines, which promote tumor growth (Ditsworth and Zong, 2004; Greten et al., 2004; Staudt, 2010). Elevated levels of IL-1 β , tumor necrosis factor α (TNF- α), and interleukin 6 (IL-6) are commonly associated with both IBD and CRC (Becker et al., 2005; Lin and Karin, 2007; Waldner et al., 2012). In particular, IL-6 and STAT3 potently stimulate colon cancer proliferation and have critical roles in colon tumor development in preclinical models (Bollrath et al., 2009; Corvinus et al., 2005; Grivennikov et al., 2009). There is also a strong correlation between local IL-6 accumulation and clinical activity of IBD in humans (Atreya and Neurath, 2005; Hyams et al., 1993).

The initial connection between IBD and the NLR family was based on the strong genetic association between NOD2/CARD15 mutations in Crohn's disease and colon cancer (Hugot et al., 2001; Kurzawski et al., 2004; Ogura et al., 2001). Mouse models of CAC have demonstrated that other NLRs, such as NLRP3, NLRP6, and NLRP12, also protect against CAC (Allen et al., 2010; Anand et al., 2012; Chen et al., 2011; Dupaul-Chicoine et al., 2010; Elinav et al., 2011; Zaki et al., 2010). The NLRP3 and NLRP6 inflammasomes appear to limit CAC primarily through the induction of IL-18, while NLRP12 reduces NF- κ B and ERK activation, hence reducing chemokines and nitric oxide that promote tumorigenesis (Allen et al., 2012; Zaki et al., 2011).

NLRX1 does not exhibit inflammasome function and is uniquely localized to the mitochondria (Moore et al., 2008; Tattoli et al., 2008). NLRX1 attenuates TRAF6, mitochondrial antiviral signaling protein (MAVS)/retinoic acid-inducible gene I (RIG-I), interferon regulatory factor 3 (IRF3), and I κ B kinase (IKK) signaling in response to viral infection and TLR signaling (Allen et al., 2011; Moore et al., 2008; Xia et al., 2011), but it is also required for the induction of reactive oxygen species in response to pathogens (Abdul-Sater et al., 2010; Tattoli et al., 2008). As a result of its impact on key signaling pathways, NLRX1 negatively regulates the expression of pro-inflammatory cytokines, including IL-6 (Allen et al., 2011), a cytokine that has a central role in CAC and is a target of therapies for the treatment of IBD (Allocca et al., 2013). A recent study reported that NLRX1 expression is reduced in patients with chronic obstructive pulmonary disease (COPD), and the absence of NLRX1 exacerbated a model of COPD (Kang et al., 2015). Thus, one of the functions of NLRX1 is to attenuate over-zealous immune responses. Therefore, elucidating the molecular

regulation and function of NLRX1 in CAC or sporadic CRC has the potential to identify novel pathways and therapeutic targets for the treatment of colon cancer.

Analyses of inflammasome NLRs in models of CAC have been well reported; however, CAC represents only 1% of CRC. By contrast, the importance of NLRs in the more prevalent sporadic colon tumors is sorely lacking. This current study identifies an important role for *Nlr1* in suppressing tumorigenesis in both CAC and sporadic colon cancer models by restricting the activation of NF- κ B, MAPK, STAT3, and IL-6 production. In contrast to most inflammasome NLRs, which function through the myeloidmonocytic hematopoietic system, NLRX1 exerts its impact primarily through non-hematopoietic cells such as colon crypt cells. The importance of NLRX1 in cells other than hematopoietic is consistent with its role in sporadic CRC modeled after familial adenomatous polyposis (FAP). FAP is a hereditary disease characterized by the development of colon polyps, attributed to the deletion of the *APC* (adenomatous polyposis coli) gene (Fodde et al., 2001). Mutations in the *APC* gene also lead to sporadic colon cancer. The *Apc^{Min/+}* mouse model has a point mutation in the *Apc* gene, which predisposes the mice to increased spontaneous intestinal polyps. This study reveals that compared to *Apc^{min/+}* controls, *Apc^{min/+}* mice lacking *Nlr1* have a dramatically increased tumor burden accompanied by increased IL-6, STAT3, β -catenin, and cathepsin B activation. Treatment of *Nlr1^{-/-}Apc^{Min/+}* mice with anti-IL6R therapy reduced STAT3 activation, decreased tumor number, and increased survival, indicating that increased IL-6 is a causative factor in tumorigenesis linked to NLRX1-deficiency. Expression analyses of clinical human colon cancer samples and meta-analysis of multiple public databases revealed that *NLRX1* expression is significantly lowered in CRC when compared to normal colon tissues. These findings indicate that the loss or reduction of NLRX1 may contribute to human colon cancers.

RESULTS

***Nlr1^{-/-}* Mice Are More Susceptible to Chronic Azoxymethane/Dextran Sodium Sulfate-Induced Colitis-Associated Colon Cancer**

To test the hypothesis that NLRX1 impacts colon tumorigenesis, *Nlr1^{-/-}* and wild-type (WT) littermates were subjected to a well-characterized CAC model that combines the genotoxic DNA-methylation agent, azoxymethane (AOM), and dextran sodium sulfate (DSS) (Neufert et al., 2007). CAC was induced by injecting a single dose of AOM, followed by three cycles of 3% DSS administration for 5 days followed by 14 days of regular drinking water, hereafter referred to as A/D treatment (Figure 1A). A/D-treated *Nlr1^{-/-}* mice exhibited statistically greater weight loss than A/D-treated wild-type mice (Figure 1B). A clinical score based on body condition, stool consistency, rectal bleeding, and the presence of blood in the stool (Allen et al., 2010) was significantly higher in *Nlr1^{-/-}* animals compared to WT controls (Figure 1C). The histologic appearance of the *Nlr1^{-/-}* colons harvested at 55 days post A/D injection showed increased total histology score (THS) (Figures 1D and 1E), which evaluates severity and extent of inflammation, epithelial defects, crypt atrophy, and mucosal dysplasia/neoplasia. *Nlr1^{-/-}*-treated colons had more widespread epithelial defects compared to controls as scored in a blinded fashion by a board-certified veterinarian pathologist (Figure 1F, see legend for a detailed description).

On day 55 after the start of A/D, colons were harvested and macroscopic polyps were counted. A/D-treated *Nlr1^{-/-}* mice exhibited significantly more polyps in the distal region of their colons compared to A/D-treated WT controls (Figure 1G). *Nlr1^{-/-}* mice also exhibited greater tumor volume compared to WT controls (Figure S1A). Mice treated with DSS or AOM alone had few, if any, polyps. Further analysis by endoscopy with a different group of mice revealed that A/D-treated *Nlr1^{-/-}* mice developed more polyps or lesions at the time of examination (day 48 of the A/D treatment course) compared to WT control mice (Figure S1B). NLRX1 attenuates cytokine expression in fibroblasts (Allen et al., 2011). To assess if this occurs in CAC, serum from A/D-treated *Nlr1^{-/-}* mice were prepared and showed significantly higher levels of IL-6, TNF- α , and IL-1 β protein than controls as determined by ELISA (Figure 1H) and greater *Il6*, *Tnf α* , and *Il1 β* RNA expression as determined by real-time PCR from colon tissues (Figure 1I). Previous reports have demonstrated the role of increased NF- κ B and ERK activation in CAC development (Greten et al., 2004). Western blot analysis revealed that colons of chronic DSS- or A/D-treated *Nlr1^{-/-}* mice had higher levels of phosphorylated I κ B α and ERK1/2 compared to WT controls (Figures 1J and 1K). Furthermore, IL-6 induces the activation of STAT3, which is dysregulated in colon cancer. Colons from A/D-treated *Nlr1^{-/-}* mice had significantly higher levels of phosphorylated STAT3 compared to WT controls (Figures 1J and 1K). These results show that NLRX1 mitigates several known tumor-promoting signaling pathways during CAC.

***Nlr1* Expression in the Non-hematopoietic Compartment Mediates Protection against Colon Tumorigenesis**

NLRX1 is widely expressed in different tissues and organs (Moore et al., 2008), hence its impact on CAC might be attributed to its expression in hematopoietic and/or non-hematopoietic cells. To address this, the following four groups of bone marrow chimeras were generated to test whether hematopoietic and/or non-hematopoietic cells were needed to protect against polyp formation: (1) irradiated WT mice that received bone marrow from WT littermates (WT > WT, control group), (2) irradiated WT control mice that received bone marrow from *Nlr1^{-/-}* donors (*Nlr1^{-/-}* > WT, hematopoietic component was *Nlr1^{-/-}*-deficient), (3) irradiated *Nlr1^{-/-}* mice that received bone marrow from *Nlr1^{-/-}* donors (*Nlr1^{-/-}* > *Nlr1^{-/-}*, global *Nlr1* deficiency), and (4) irradiated *Nlr1^{-/-}* mice that received bone marrow from WT donors (WT > *Nlr1^{-/-}*, non-hematopoietic compartment was *Nlr1^{-/-}*-deficient). All reconstituted mice were treated with A/D and monitored for 55 days. Within the first 10–15 days post A/D treatment, almost 50% of the *Nlr1^{-/-}* > *Nlr1^{-/-}* and WT > *Nlr1^{-/-}* mice died (Figure 2A). Of the mice that survived, a clinical score was assessed. WT > *Nlr1^{-/-}* and *Nlr1^{-/-}* > *Nlr1^{-/-}* groups showed increased clinical scores compared to the WT > WT controls and the *Nlr1^{-/-}* > WT groups at all three indicated time points (Figure 2B). WT > *Nlr1^{-/-}* and *Nlr1^{-/-}* > *Nlr1^{-/-}* groups had an increase in THS when compare to *Nlr1^{-/-}* > WT group and WT > WT controls (Figures 2C and 2D). *Nlr1^{-/-}* > *Nlr1^{-/-}* had a higher THS possibly due to the fact that NLRX1 is expressed in many different cell types (Figure 2D). Similar to findings with non-chimeric *Nlr1^{-/-}* mice, the *Nlr1^{-/-}* > *Nlr1^{-/-}* group had a higher number of colonic polyps than WT > WT controls (Figure 2E). WT > *Nlr1^{-/-}* mice showed significantly higher numbers of polyps than the WT > WT and *Nlr1^{-/-}* > WT mice (Figure 2E). Colonic polyp numbers in

Nlr1^{-/-} > WT mice were not significantly different from WT > WT controls. *Nlr1^{-/-}* > *Nlr1^{-/-}* and WT > *Nlr1^{-/-}* mice, but not *Nlr1^{-/-}* > WT mice, had significantly increased tumor volume compared to WT > WT mice (Figure 2F). Additionally, phosphorylated STAT3 was higher in *Nlr1^{-/-}* > *Nlr1^{-/-}* and WT > *Nlr1^{-/-}* mice compared to *Nlr1^{-/-}* > WT and WT > WT mice (Figure 2G). A composite of three experiments confirmed these results (Figure 2H). These results indicate that the presence of *Nlr1* in the non-hematopoietic compartment is primarily required to limit A/D-induced tumorigenesis and STAT3 activation.

Loss of *Nlr1* in the *Apc^{min/+}* Model of Sporadic CRC Leads to Increased Mortality and Tumor Burden

The above data indicate a contribution of *Nlr1*-deficiency from the non-hematopoietic compartment during CAC pathogenesis. However, the majority of colon cancers are not associated with CAC. Therefore, we explored the role of NLRX1 in a model of sporadic colon cancer. *APC* mutations are found in ~85% of human colon cancers or precancerous adenomas, and the loss of *APC* in epithelial cells is sufficient to drive intestinal tumorigenesis (Kinzler and Vogelstein, 1996; Schwitalla et al., 2013). *Apc^{min/+}* mice have a germline mutation in the *APC* gene and develop spontaneous polyps (Fodde et al., 2001). Usually, *Apc^{min/+}* mice become moribund within 168 days of age due to complications from intestinal tumors (Heyer et al., 1999). To explore the role of NLRX1 in a model of sporadic colon cancer, *Nlr1^{-/-}* mice were bred with *Apc^{min/+}* mice to test if the loss of *Nlr1* affected spontaneous tumor development and lethality. Survival of *Nlr1^{-/-}Apc^{min/+}* mice was dramatically decreased when compared to *Apc^{min/+}* littermate controls (Figure 3A). Mice were monitored and harvested at 42, 84, and 168 days of age to elucidate potential factors of early mortality (Figure S2A). At 168 days, *Nlr1^{-/-}Apc^{min/+}* mice exhibited obvious signs of hunched back (Figure S2B), which correlated with an increase in clinical score (Figure 3B). *Apc^{min/+}* and *Nlr1^{-/-}Apc^{min/+}* mice did not differ in body weight at 84 to 168 days, although there was a slight and statistically significant difference between *Nlr1^{-/-}* and WT mice at 42 days (Figure S2C). Macroscopic analysis of unstained colons and colons stained by Alcian blue revealed that *Nlr1^{-/-}Apc^{min/+}* colons had increased polyps (Figure 3C). The numbers of visible polyps were quantified at three different time points. At 42 days of age, colonic (Figure 3D) polyp numbers were not significantly different among the four groups. However, at 84 days and 168 days of age, a modest number of polyps appeared in *Apc^{min/+}* mice as reported in the literature (Heyer et al., 1999), while *Nlr1^{-/-}Apc^{min/+}* mice developed significantly more visible polyps in their colons compared to *Apc^{min/+}* mice (Figure 3D). In addition, *Nlr1^{-/-}Apc^{min/+}* colons had larger tumor volume when compared to *Apc^{min/+}* colons (Figure 3E). These results suggest that NLRX1 attenuates both polyp number and tumor volume during sporadic colon cancer.

NLRX1 Attenuates Aberrant Cellular Proliferation and Disease Progression in the *APC^{min/+}* Mouse Tumor Model

Histological analysis of H&E-stained colons from 168-day-old *Nlr1^{-/-}Apc^{min/+}* mice revealed a higher THS marked by more severe histologic lesions, including increased incidence of colonic dysplasia and neoplasm compared to similar-aged *Apc^{min/+}* or *Nlr1^{-/-}* mice (Figure 4A, see figure legend for a detailed description of the histology). We also

observed a higher rate of distal inflammation in the colons of *Nlr1^{-/-}Apc^{min/+}* mice (Figure 4B). In addition, we observed no difference in the percentage of cleaved caspase 3, a marker of apoptosis, between WT and *Nlr1^{-/-}* (Figure 4C) while we saw significantly higher levels of Ki67⁺ cells in the basal end of colon crypts in *Nlr1^{-/-}* and *Nlr1^{-/-}Apc^{min/+}* mice compared to wild-type and *Apc^{min/+}* mice, which is an indicator of increased proliferation (Figures 4D and 4E). APC controls the stability of β -catenin, a key regulator of Wnt signaling, stem cell renewal, cell fate, and growth (Clevers and Nusse, 2012). Additionally, increased cytoplasmic β -catenin is a marker of carcinogenesis (Fodde et al., 2001). Immunohistochemical staining of *Nlr1^{-/-}Apc^{min/+}* tumors showed increased β -catenin compared to *Apc^{min/+}* controls (Figure 4F).

Our findings indicate that STAT3 was hyperactivated in the absence of NLRX1 (Figure 1J). STAT3 is known to activate cathepsin-B, which is involved in the oncogenesis and metastasis of human cancers and it is upregulated in dysplastic adenomas and colorectal carcinoma (Ding et al., 2014; Kuester et al., 2008). Ex vivo imaging of colons of *Nlr1^{-/-}Apc^{min/+}* mice, *Apc^{min/+}*, *Nlr1^{-/-}*, and WT controls injected with a cathepsin B-inducible fluorescence probe (Prosense 680) (Ding et al., 2014; Gounaris et al., 2013) revealed significantly higher fluorescence in colons of *Nlr1^{-/-}Apc^{min/+}* versus *Apc^{min/+}* mice, which is indicative of increased cathepsin B activity in the *Nlr1^{-/-}Apc^{min/+}* mice (Figure 4G). Colons of *Nlr1^{-/-}* and WT littermates showed minimal cathepsin B signals (Figure 4G). This result indicates that cathepsin B activity is enhanced in *Nlr1^{-/-}Apc^{min/+}* mice.

NLRX1 Attenuates Tumor-Promoting Signaling Pathways in Colon Crypts during the *Apc^{min/+}* Model of Spontaneous CRC

To assess whether the presence of NLRX1 attenuated key tumor-promoting pathways in the *Apc^{min/+}* model, colons were isolated and analyzed by western blot. *Nlr1^{-/-}Apc^{min/+}* colons had higher levels of phosphorylated p65, I κ B α , JNK1/2, and ERK1/2 at 84 (Figure 5A) and 168 (Figure 5B) days of age compared to *Nlr1^{-/-}*, *Apc^{min/+}*, and WT mice. Phosphorylated STAT3 was also elevated in *Nlr1^{-/-}Apc^{min/+}* colons (Figures 5A and 5B). Since *Nlr1^{-/-}Apc^{min/+}* had increased levels of Ki67⁺ in their colon crypt (Figure 4D), we isolated these cells to determine the impact of NLRX1-deficiency. These cells were EpCAM^{hi} and CD45^{lo} (Figure S3). *Nlr1^{-/-}Apc^{min/+}* colon crypts from 84-day-old mice had higher levels of phosphorylated p65, ERK1/2, and STAT3 (Figure 5C) than controls. Since STAT3 can be activated by the key tumor-promoting cytokine, IL-6, *Il6* transcript was measured by qPCR, and it was significantly increased in *Nlr1^{-/-}Apc^{min/+}* colons (Figure 5D). In contrast, levels of *Tnf α* and *Il1 β* were not significantly different between *Apc^{min/+}* and *Nlr1^{-/-}Apc^{min/+}* colons (Figure 5D). ELISA analysis verified significantly higher levels of IL-6 protein produced by colonic samples isolated from *Nlr1^{-/-}Apc^{min/+}* animals compared to *Apc^{min/+}* mice, but no difference in IL-1 β and TNF- α , which was below detection (Figure 5E). Taken together, these results indicate that the loss of NLRX1-activated multiple pathways that contribute to tumor development or progression.

Anti-IL6R Therapy Significantly Decreases Tumor Burden and STAT3 Activity in the *Nlr1-1-Apc^{min/+}* Animals

To assess whether the pathways delineated above contributed to the mechanism by which NLRX1 suppressed tumor growth, we directly assessed the role of elevated IL-6 in *Nlr1-1-Apc^{min/+}* animals with antibodies against IL-6 receptor. WT, *Nlr1-1-^{-/-}*, *Apc^{min/+}*, and *Nlr1-1-^{-/-}Apc^{min/+}* animals were injected with 20 µg/ml of anti-IL6R per mouse biweekly for 10 weeks. Cumulative clinical score revealed that *Nlr1-1-^{-/-}Apc^{min/+}* mice on anti-IL6R treatment had a significantly lowered clinical score compared to the untreated (UT) *Nlr1-1-^{-/-}Apc^{min/+}* group (Figure 6A). Anti-IL6R-treated *Nlr1-1-^{-/-}Apc^{min/+}* mice showed significant weight gain compared to UT controls, while anti-IL6R-treated WT, *Nlr1-1-^{-/-}*, and *Apc^{min/+}* showed a modest, but insignificant weight loss compared to their UT controls (Figure 6B). After 10 weeks of anti-IL-6R therapy, colons were harvested and macroscopic polyps were counted. Anti-IL6R-treated *Nlr1-1-^{-/-}Apc^{min/+}* animals exhibited significantly less polyps in the distal region of their colons in comparison to UT *Nlr1-1-^{-/-}Apc^{min/+}* (Figures 6C and 6D). Western blot showed a significant decrease of phosphorylated STAT3 in anti-IL6R-treated *Nlr1-1-^{-/-}Apc^{min/+}* animals in comparison to UT animals (Figure 6E). STAT3 is well documented to regulate the initial events of tumor development, progression, and invasiveness (Waldner et al., 2012) (Figure 6F) and decreased levels of phosphorylated STAT3 observed in anti-IL6R-treated *Nlr1-1-^{-/-}Apc^{min/+}* animals correlated positively with decreased polyp numbers (Figures 6D and 6F). Thus, these results indicate that increased IL-6 found in *Nlr1-1-^{-/-}Apc^{min/+}* played a causative role in increased polyp formation and heightened STAT3 activation.

NLRX1 Expression Is Reduced in Colorectal Cancer Based on Analysis of the Oncomine Platform and Newly Isolated Clinical Samples

To examine the relevance of the data in preclinical models to human colon cancer, the levels of *NLRX1* expression in human CRC was subjected to bioinformatics mining using the Oncomine Platform database. This was followed by an examination of newly isolated clinical samples from a Chinese Cohort. Oncomine Platform is an online assembly of microarrays. We analyzed five databases (listed in the Experimental Procedures) that contained information regarding *NLRX1* expression. We first analyzed the Cancer Genome Atlas (TCGA) database, which is the most comprehensive set containing 215 patient and 22 control samples (Cancer Genome Atlas, 2012). This database showed that the expression of *NLRX1* transcript was significantly decreased in colorectal cancer (Figure 7A). Next, we evaluated the expression levels of *NLRX1* transcript at various stages of cancer progression using the TCGA database (Figure 7B). CRC cases were staged according to the staging system determined by the American Joint Committee on Cancer (AJCC) and also known as the tumor-node-metastasis (TNM) system. In stage I, the tumor has spread beyond the inner lining of the colon to the second and third layers of the colon. In stage II, the tumor has spread to the muscle wall of the colon. In stage III, the cancer has metastasized to lymph nodes. In stage IV, the cancer has metastasized to secondary areas of the body such as the liver or lung. This analysis shows that *NLRX1* expression was significantly higher in healthy controls versus all four CRC stages (Figure 7B). Next, we confirmed these findings using four smaller databases within the Oncomine Platform. Significantly lower expression of *NLRX1* was detected in CRC samples in all four databases (Figure 7C). Thus, the composite

data from five public databases support the conclusion that *NLRX1* expression is statistically lower in CRC than in healthy colons.

Public database typically do not provide detailed information regarding the patients. Thus, we analyzed mRNA isolated from 40 formalin-fixed and paraffin-embedded (FFPE) CRC samples plus 40 adjacent normal tissues obtained from a Chinese patient cohort for the expression of *NLRX1*. The patients selected had not received any chemotherapy or radiotherapy prior to colonic resection. In agreement with Figure 7A, *NLRX1* transcripts were significantly reduced within the CRC samples relative to healthy tissues (Figure 7D). The combined data collected from multiple public databases and an additional cohort of human clinical samples provides overwhelming clinical evidence that *NLRX1* gene expression is reduced in human CRC in comparison to healthy colons, further indicating a critical role for NLRX1 in limiting CRC.

DISCUSSION

The link between cancer and a number of key signaling pathways is well established (Coussens and Werb, 2002). Elevated NF- κ B signaling can de-differentiate intestinal epithelial cells that eventually acquire stem-like properties and tumor-initiating capacity (Shaked et al., 2012). NF- κ B also facilitates Wnt-driven proliferation of intestinal stem cells, which leads to CRC (Myant et al., 2013; Schwitalla et al., 2013). MAPK regulates intestinal cell proliferation and epithelial differentiation and promotes progression and oncogenesis of human CRC (Dhillon et al., 2007; Lee et al., 2010; Taupin and Podolsky, 1999). NF- κ B and STAT3 cooperatively regulate a number of target genes regulating cell cycle and proliferation (Lee et al., 2009; Yang et al., 2007). This work shows that NLRX1 serves as a checkpoint of these multiple critical cancer-promoting pathways to maintain a homeostatic, noncancerous state.

A previous study of NLRX1 in a model that used AOM alone, which is not known to strongly induce tumorigenesis, and a model that involved a short course (3-day) of AOM-DSS treatment, which is unlikely to induce full tumorigenesis, has resulted in conflicting findings regarding the role of NLRX1 (Soares et al., 2014). In contrast, the current study is distinguished by several unique features First, NLRX1 uniformly suppressed colon tumorigenesis in both CAC and sporadic colon cancer models. Second, the loss of *Nlr1* expression led to heightened IL-6 production and activated STAT3, which are key regulatory pathways in colon cancer that have not been connected to NLR function in tumors. Enhanced NF- κ B and ERK activity are known to enhance levels of IL-6, which can lead to STAT3 activation resulting in increased oncogenesis (Corvinus et al., 2005). Cross talk between STAT3 and β -catenin have been documented in different cancers (Armanious et al., 2010; Ibrahim et al., 2014), and STAT3 can also enhance cathepsin B (Dauer et al., 2005), which enhances cancer progression and cell proliferation. Since cathepsin B and β -catenin activity are heightened in *Nlr1*^{-/-} *Apc*^{min/+} mice, inhibitors of these two proteins may be useful in targeting human CRCs with low *NLRX1* expression. Third, while other NLRs such as NLRP3 exert their impact primarily through the hematopoietic compartment, NLRX1 exerts its impact on tumorigenesis mostly via the non-hematopoietic compartment such as colon crypts. Fourth, anti-IL6R therapy effectively decreased tumorigenesis and STAT3

activation in *Nlr1^{-/-}Apc^{min/+}* animals. Finally, NLRX1 is also reduced in multiple human CRC patient cohorts, which confers translational relevance to these findings and supports the concept that NLRX1 may serve as a checkpoint against human colon cancer. The discovery of reduced *NLRX1* in human CRC further suggests that *NLRX1* expression may be used as a biomarker of CAC or CRC (Thorsteinsdottir et al., 2011). This finding also has implications for personalized therapy. For example, inhibitors of STAT3 or IL-6, which are Food and Drug Administration (FDA)-approved for other diseases, might be repurposed for controlling human CRCs that have low *NLRX1* expression. Based on the findings in this and previous reports, a working model of how NLRX1 affects tumorigenesis is shown in Figure 6F.

In summary, this report finds that the presence of NLRX1 limits activation of key signaling pathways leading to NF- κ B, MAPK, IL-6, and STAT3 activation, which promote various aspects of tumor development. The loss of NLRX1 creates a microenvironment that potentiates the development of tumors in both colitis-associated and sporadic models of CRC. A possible impact is that NLRX1 affects tumor-promoting signals via changes in the microbiome, which would be an important future investigation.

EXPERIMENTAL PROCEDURES

Animals

All studies were conducted in accordance with IACUC guidelines of the University of North Carolina (UNC) at Chapel Hill and NIH guide for the Care and Use of Laboratory Animals. All experiments were performed under SPF conditions using either 6- or 8-week-old male mice or with age as indicated. C57BL/6 (wild-type mice) and *Apc^{min/+}* mice originated from Jackson Laboratories and were maintained at UNC Chapel Hill for more than nine generations. *Nlr1^{-/-}* mice on the C57BL/6 background have been described previously (Moore et al., 2008). *Nlr1^{-/-}* mice were crossed with *Apc^{min/+}* mice to generate *Nlr1^{-/-}Apc^{min/+}* mice. Littermates were used as indicated. See the Supplemental Experimental Procedures for colitis and colon cancer models, generation of radiation bone marrow chimeras, and assessment of colon polyps and histopathology.

Assays

Isolation of RNA, tissue extracts, and soluble protein and biochemical and molecular analyses and molecular imaging of proteases are described in the Supplemental Experimental Procedures.

Bioinformatics and Experimental Analysis of *NLRX1* Expression in Human CRC

Microarray studies from the OncoPrint Platform containing data describing *NLRX1* expression in CRC and the collection and processing of human CRC specimens are described in the Supplemental Experimental Procedures.

Statistics

All results are presented as the mean \pm SEM. Significance between two groups was assessed by the Student's two-tailed t test. Datasets that had more than two sets of data for analysis

were analyzed by ANOVA with Tukey–Kramer HSD post test for multiple comparisons to determine significance. The product limit method of Kaplan–Meier was utilized for generating the survival curves, which were compared using the log rank test. See the Supplemental Experimental Procedures for statistics used with clinical human samples.

Supplementary Material

Refer to Web version on PubMed Central for supplementary material.

ACKNOWLEDGMENTS

This project was supported in part by NIH grants CA156330 (to J.P.-Y.T. and A.A.K.), AI029564, DK094779, 5-T32-LCCC (to LCCC), T32-DK007737 (to UNC Gastroenterology Research Training), DK047769 (to S.D. and P.K.L.), and F32-DK098916 (to A.D.T.). J.E.W. was supported by the American Cancer Society (PF-13-401-01-TBE). Animal histopathology was performed within the LCCC Animal Histopathology Core Facility at UNC, supported in part by the National Cancer Institute (CA16086).

REFERENCES

- Abdul-Sater AA, Saïd-Sadier N, Lam VM, Singh B, Pettengill MA, Soares F, Tattoli I, Lipinski S, Girardin SE, Rosenstiel P, Ojcius DM. Enhancement of reactive oxygen species production and chlamydial infection by the mitochondrial Nod-like family member NLRX1. *J. Biol. Chem.* 2010; 285:41637–41645. [PubMed: 20959452]
- Allen IC, TeKippe EM, Woodford RM, Uronis JM, Holl EK, Rogers AB, Herfarth HH, Jobin C, Ting JP. The NLRP3 inflammasome functions as a negative regulator of tumorigenesis during colitis-associated cancer. *J. Exp. Med.* 2010; 207:1045–1056. [PubMed: 20385749]
- Allen IC, Moore CB, Schneider M, Lei Y, Davis BK, Scull MA, Gris D, Roney KE, Zimmermann AG, Bowzard JB, et al. NLRX1 protein attenuates inflammatory responses to infection by interfering with the RIG-IMAVS and TRAF6-NF- κ B signaling pathways. *Immunity.* 2011; 34:854–865. [PubMed: 21703540]
- Allen IC, Wilson JE, Schneider M, Lich JD, Roberts RA, Arthur JC, Woodford RM, Davis BK, Uronis JM, Herfarth HH, et al. NLRP12 suppresses colon inflammation and tumorigenesis through the negative regulation of noncanonical NF- κ B signaling. *Immunity.* 2012; 36:742–754. [PubMed: 22503542]
- Allocca M, Jovani M, Fiorino G, Schreiber S, Danese S. Anti-IL-6 treatment for inflammatory bowel diseases: next cytokine, next target. *Curr. Drug Targets.* 2013; 14:1508–1521. [PubMed: 24102406]
- Anand PK, Malireddi RK, Lukens JR, Vogel P, Bertin J, Lamkanfi M, Kanneganti TD. NLRP6 negatively regulates innate immunity and host defence against bacterial pathogens. *Nature.* 2012; 488:389–393. [PubMed: 22763455]
- Armanious H, Gelebart P, Mackey J, Ma Y, Lai R. STAT3 up-regulates the protein expression and transcriptional activity of b-catenin in breast cancer. *Int. J. Clin. Exp. Pathol.* 2010; 3:654–664. [PubMed: 20830236]
- Atreya R, Neurath MF. Involvement of IL-6 in the pathogenesis of inflammatory bowel disease and colon cancer. *Clin. Rev. Allergy Immunol.* 2005; 28:187–196. [PubMed: 16129903]
- Bailey CE, Hu CY, You YN, Bednarski BK, Rodriguez-Bigas MA, Skibber JM, Cantor SB, Chang GJ. Increasing disparities in the age-related incidences of colon and rectal cancers in the United States, 1975–2010. *JAMA Surg.* 2015; 150:17–22. [PubMed: 25372703]
- Becker C, Fantini MC, Wirtz S, Nikolaev A, Lehr HA, Galle PR, Rose-John S, Neurath MF. IL-6 signaling promotes tumor growth in colorectal cancer. *Cell Cycle.* 2005; 4:217–220. [PubMed: 15655344]
- Ben-Neriah Y, Karin M. Inflammation meets cancer, with NF- κ B as the matchmaker. *Nat. Immunol.* 2011; 12:715–723. [PubMed: 21772280]
- Bollrath J, Pheesse TJ, von Burstin VA, Putoczki T, Bennecke M, Bateman T, Nebelsiek T, Lundgren-May T, Canli O, Schwitalla S, et al. gp130-mediated Stat3 activation in enterocytes regulates cell

- survival and cell-cycle progression during colitis-associated tumorigenesis. *Cancer Cell*. 2009; 15:91–102. [PubMed: 19185844]
- Cancer Genome Atlas, N.; Cancer Genome Atlas Network. Comprehensive molecular characterization of human colon and rectal cancer. *Nature*. 2012; 487:330–337. [PubMed: 22810696]
- Chen GY, Liu M, Wang F, Bertin J, Núñez G. A functional role for Nlrp6 in intestinal inflammation and tumorigenesis. *J. Immunol*. 2011; 186:7187–7194. [PubMed: 21543645]
- Clevers H, Nusse R. Wnt/b-catenin signaling and disease. *Cell*. 2012; 149:1192–1205. [PubMed: 22682243]
- Corvinus FM, Orth C, Moriggl R, Tsareva SA, Wagner S, Pfitzner EB, Baus D, Kaufmann R, Huber LA, Zatloukal K, et al. Persistent STAT3 activation in colon cancer is associated with enhanced cell proliferation and tumor growth. *Neoplasia*. 2005; 7:545–555. [PubMed: 16036105]
- Coussens LM, Werb Z. Inflammation and cancer. *Nature*. 2002; 420:860–867. [PubMed: 12490959]
- Dauer DJ, Ferraro B, Song L, Yu B, Mora L, Buettner R, Enkemann S, Jove R, Haura EB. Stat3 regulates genes common to both wound healing and cancer. *Oncogene*. 2005; 24:3397–3408. [PubMed: 15735721]
- Dhillon AS, Hagan S, Rath O, Kolch W. MAP kinase signalling pathways in cancer. *Oncogene*. 2007; 26:3279–3290. [PubMed: 17496922]
- Ding S, Blue RE, Morgan DR, Lund PK. Comparison of multiple enzyme activatable near-infrared fluorescent molecular probes for detection and quantification of inflammation in murine colitis models. *Inflamm. Bowel Dis*. 2014; 20:363–377. [PubMed: 24374874]
- Ditsworth D, Zong WX. NF-kappaB: key mediator of inflammation-associated cancer. *Cancer Biol. Ther*. 2004; 3:1214–1216. [PubMed: 15611628]
- Dupaul-Chicoine J, Yeretssian G, Doiron K, Bergstrom KS, McIntire CR, LeBlanc PM, Meunier C, Turbide C, Gros P, Beauchemin N, et al. Control of intestinal homeostasis, colitis, and colitis-associated colorectal cancer by the inflammatory caspases. *Immunity*. 2010; 32:367–378. [PubMed: 20226691]
- Elinav E, Strowig T, Kau AL, Henao-Mejia J, Thaiss CA, Booth CJ, Peaper DR, Bertin J, Eisenbarth SC, Gordon JI, Flavell RA. NLRP6 inflammasome regulates colonic microbial ecology and risk for colitis. *Cell*. 2011; 145:745–757. [PubMed: 21565393]
- Elinav E, Nowarski R, Thaiss CA, Hu B, Jin C, Flavell RA. Inflammation-induced cancer: crosstalk between tumours, immune cells and microorganisms. *Nat. Rev. Cancer*. 2013; 13:759–771. [PubMed: 24154716]
- Fleming M, Ravula S, Tatishev SF, Wang HL. Colorectal carcinoma: Pathologic aspects. *J. Gastrointest. Oncol*. 2012; 3:153–173. [PubMed: 22943008]
- Fodde R, Smits R, Clevers H. APC, signal transduction and genetic instability in colorectal cancer. *Nat. Rev. Cancer*. 2001; 1:55–67. [PubMed: 11900252]
- Gounaris E, Martin J, Ishihara Y, Khan MW, Lee G, Sinh P, Chen EZ, Angarone M, Weissleder R, Khazaie K, Barrett TA. Fluorescence endoscopy of cathepsin activity discriminates dysplasia from colitis. *Inflamm. Bowel Dis*. 2013; 19:1339–1345. [PubMed: 23591598]
- Greten FR, Eckmann L, Greten TF, Park JM, Li ZW, Egan LJ, Kagnoff MF, Karin M. IKKbeta links inflammation and tumorigenesis in a mouse model of colitis-associated cancer. *Cell*. 2004; 118:285–296. [PubMed: 15294155]
- Grivennikov S, Karin E, Terzic J, Mucida D, Yu GY, Vallabhapurapu S, Scheller J, Rose-John S, Cheroutre H, Eckmann L, Karin M. IL-6 and Stat3 are required for survival of intestinal epithelial cells and development of colitis-associated cancer. *Cancer Cell*. 2009; 15:103–113. [PubMed: 19185845]
- Hayden MS, Ghosh S. NF-κB in immunobiology. *Cell Res*. 2011; 21:223–244. [PubMed: 21243012]
- Heyer J, Yang K, Lipkin M, Edelmann W, Kucherlapati R. Mouse models for colorectal cancer. *Oncogene*. 1999; 18:5325–5333. [PubMed: 10498885]
- Hugot J-P, Chamaillard M, Zouali H, Lesage S, Cézard J-P, Belaiche J, Almer S, Tysk C, O'Morain CA, Gassull M, et al. Association of NOD2 leucine-rich repeat variants with susceptibility to Crohn's disease. *Nature*. 2001; 411:599–603. [PubMed: 11385576]

- Hyams JS, Fitzgerald JE, Treem WR, Wyzga N, Kreutzer DL. Relationship of functional and antigenic interleukin 6 to disease activity in inflammatory bowel disease. *Gastroenterology*. 1993; 104:1285–1292. [PubMed: 7683293]
- Ibrahim S, Al-Ghamdi S, Baloch K, Muhammad B, Fadhil W, Jackson D, Nateri AS, Ilyas M. STAT3 paradoxically stimulates b-catenin expression but inhibits b-catenin function. *Int. J. Exp. Pathol*. 2014; 95:392–400. [PubMed: 25348333]
- Kang MJ, Yoon CM, Kim BH, Lee CM, Zhou Y, Sauler M, Homer R, Dhamija A, Boffa D, West AP, et al. Suppression of NLRX1 in chronic obstructive pulmonary disease. *J. Clin. Invest*. 2015; 125:2458–2462. [PubMed: 25938787]
- Kinzler KW, Vogelstein B. Lessons from hereditary colorectal cancer. *Cell*. 1996; 87:159–170. [PubMed: 8861899]
- Kuester D, Lippert H, Roessner A, Krueger S. The cathepsin family and their role in colorectal cancer. *Pathol. Res. Pract*. 2008; 204:491–500. [PubMed: 18573619]
- Kurzwaski G, Suchy J, Klady J, Grabowska E, Mierzejewski M, Jakubowska A, Debniak T, Cybulski C, Kowalska E, Szych Z, et al. The NOD2 3020insC mutation and the risk of colorectal cancer. *Cancer Res*. 2004; 64:1604–1606. [PubMed: 14996717]
- Lee H, Herrmann A, Deng J-H, Kujawski M, Niu G, Li Z, Forman S, Jove R, Pardoll DM, Yu H. Persistently activated Stat3 maintains constitutive NF-kappaB activity in tumors. *Cancer Cell*. 2009; 15:283–293. [PubMed: 19345327]
- Lee SH, Hu LL, Gonzalez-Navajas J, Seo GS, Shen C, Brick J, Herdman S, Varki N, Corr M, Lee J, Raz E. ERK activation drives intestinal tumorigenesis in Apc(min/+) mice. *Nat. Med*. 2010; 16:665–670. [PubMed: 20473309]
- Lin WW, Karin M. A cytokine-mediated link between innate immunity, inflammation, and cancer. *J. Clin. Invest*. 2007; 117:1175–1183. [PubMed: 17476347]
- Moore CB, Bergstralh DT, Duncan JA, Lei Y, Morrison TE, Zimmermann AG, Accavitti-Loper MA, Madden VJ, Sun L, Ye Z, et al. NLRX1 is a regulator of mitochondrial antiviral immunity. *Nature*. 2008; 451:573–577. [PubMed: 18200010]
- Myant KB, Cammareri P, McGhee EJ, Ridgway RA, Huels DJ, Cordero JB, Schwitalla S, Kalna G, Ogg EL, Athineos D, et al. ROS production and NF-κB activation triggered by RAC1 facilitate WNT-driven intestinal stem cell proliferation and colorectal cancer initiation. *Cell Stem Cell*. 2013; 12:761–773. [PubMed: 23665120]
- Neufert C, Becker C, Neurath MF. An inducible mouse model of colon carcinogenesis for the analysis of sporadic and inflammation-driven tumor progression. *Nat. Protoc*. 2007; 2:1998–2004. [PubMed: 17703211]
- O'Shea JJ, Holland SM, Staudt LM. JAKs and STATs in immunity, immunodeficiency, and cancer. *N. Engl. J. Med*. 2013; 368:161–170. [PubMed: 23301733]
- Ogura Y, Bonen DK, Inohara N, Nicolae DL, Chen FF, Ramos R, Britton H, Moran T, Karaliuskas R, Duerr RH, et al. A frameshift mutation in NOD2 associated with susceptibility to Crohn's disease. *Nature*. 2001; 411:603–606. [PubMed: 11385577]
- Rogler G. Chronic ulcerative colitis and colorectal cancer. *Cancer Lett*. 2014; 345:235–241. [PubMed: 23941831]
- Schwitalla S, Fingerle AA, Cammareri P, Nebelsiek T, Göktuna SI, Ziegler PK, Canli O, Heijmans J, Huels DJ, Moreaux G, et al. Intestinal tumorigenesis initiated by dedifferentiation and acquisition of stem-cell-like properties. *Cell*. 2013; 152:25–38. [PubMed: 23273993]
- Sebolt-Leopold JS, Herrera R. Targeting the mitogen-activated protein kinase cascade to treat cancer. *Nat. Rev. Cancer*. 2004; 4:937–947. [PubMed: 15573115]
- Shaked H, Hofseth LJ, Chumanevich A, Chumanevich AA, Wang J, Wang Y, Taniguchi K, Guma M, Shenouda S, Clevers H, et al. Chronic epithelial NF-κB activation accelerates APC loss and intestinal tumor initiation through iNOS up-regulation. *Proc. Natl. Acad. Sci. USA*. 2012; 109:14007–14012. [PubMed: 22893683]
- Siegel R, Naishadham D, Jemal A. Cancer statistics, 2013. *CA Cancer J. Clin*. 2013; 63:11–30. [PubMed: 23335087]

- Soares F, Tattoli I, Rahman MA, Robertson SJ, Belcheva A, Liu D, Streutker C, Winer S, Winer DA, Martin A, et al. The mitochondrial protein NLRX1 controls the balance between extrinsic and intrinsic apoptosis. *J. Biol. Chem.* 2014; 289:19317–19330. [PubMed: 24867956]
- Staudt LM. Oncogenic activation of NF-kappaB. *Cold Spring Harb. Perspect. Biol.* 2010; 2:a000109. [PubMed: 20516126]
- Takeuchi O, Akira S. Pattern recognition receptors and inflammation. *Cell.* 2010; 140:805–820. [PubMed: 20303872]
- Tattoli I, Carneiro LA, Jéhanno M, Magalhaes JG, Shu Y, Philpott DJ, Arnoult D, Girardin SE. NLRX1 is a mitochondrial NOD-like receptor that amplifies NF-kappaB and JNK pathways by inducing reactive oxygen species production. *EMBO Rep.* 2008; 9:293–300. [PubMed: 18219313]
- Taupin D, Podolsky DK. Mitogen-activated protein kinase activation regulates intestinal epithelial differentiation. *Gastroenterology.* 1999; 116:1072–1080. [PubMed: 10220499]
- Terzi J, Grivennikov S, Karin E, Karin M. Inflammation and colon cancer. *Gastroenterology.* 2010; 138:2101–2114. e5. [PubMed: 20420949]
- Thorsteinsdottir S, Gudjonsson T, Nielsen OH, Vainer B, Seidelin JB. Pathogenesis and biomarkers of carcinogenesis in ulcerative colitis. *Nat. Rev. Gastroenterol. Hepatol.* 2011; 8:395–404. [PubMed: 21647200]
- Waldner MJ, Foersch S, Neurath MF. Interleukin-6—a key regulator of colorectal cancer development. *Int. J. Biol. Sci.* 2012; 8:1248–1253. [PubMed: 23136553]
- Wullaert A, Bonnet MC, Pasparakis M. NF-κB in the regulation of epithelial homeostasis and inflammation. *Cell Res.* 2011; 21:146–158. [PubMed: 21151201]
- Xia X, Cui J, Wang HY, Zhu L, Matsueda S, Wang Q, Yang X, Hong J, Songyang Z, Chen ZJ, Wang RF. NLRX1 negatively regulates TLR-induced NF-κB signaling by targeting TRAF6 and IKK. *Immunity.* 2011; 34:843–853. [PubMed: 21703539]
- Yang J, Liao X, Agarwal MK, Barnes L, Auron PE, Stark GR. Unphosphorylated STAT3 accumulates in response to IL-6 and activates transcription by binding to NFkappaB. *Genes Dev.* 2007; 21:1396–1408. [PubMed: 17510282]
- Yashiro M. Ulcerative colitis-associated colorectal cancer. *World J. Gastroenterol.* 2014; 20:16389–16397. [PubMed: 25469007]
- Zaki MH, Boyd KL, Vogel P, Kastan MB, Lamkanfi M, Kanneganti TD. The NLRP3 inflammasome protects against loss of epithelial integrity and mortality during experimental colitis. *Immunity.* 2010; 32:379–391. [PubMed: 20303296]
- Zaki MH, Vogel P, Malireddi RK, Body-Malapel M, Anand PK, Bertin J, Green DR, Lamkanfi M, Kanneganti TD. The NOD-like receptor NLRP12 attenuates colon inflammation and tumorigenesis. *Cancer Cell.* 2011; 20:649–660. [PubMed: 22094258]

Highlights

- NLRX1 mitigates tumorigenesis in a genetic model of sporadic colon cancer, *APC^{min/+}*
- *Nlr1^{-/-}* colons have increased activation of tumor inducing STAT3, NFκB, MAPK, and IL6
- Anti-IL6R therapy reduces mortality and tumor development in *Nlr1^{-/-}* *APC^{min/+}* mice
- Human colon tumors exhibit significantly lower levels of NLRX1 in multiple datasets

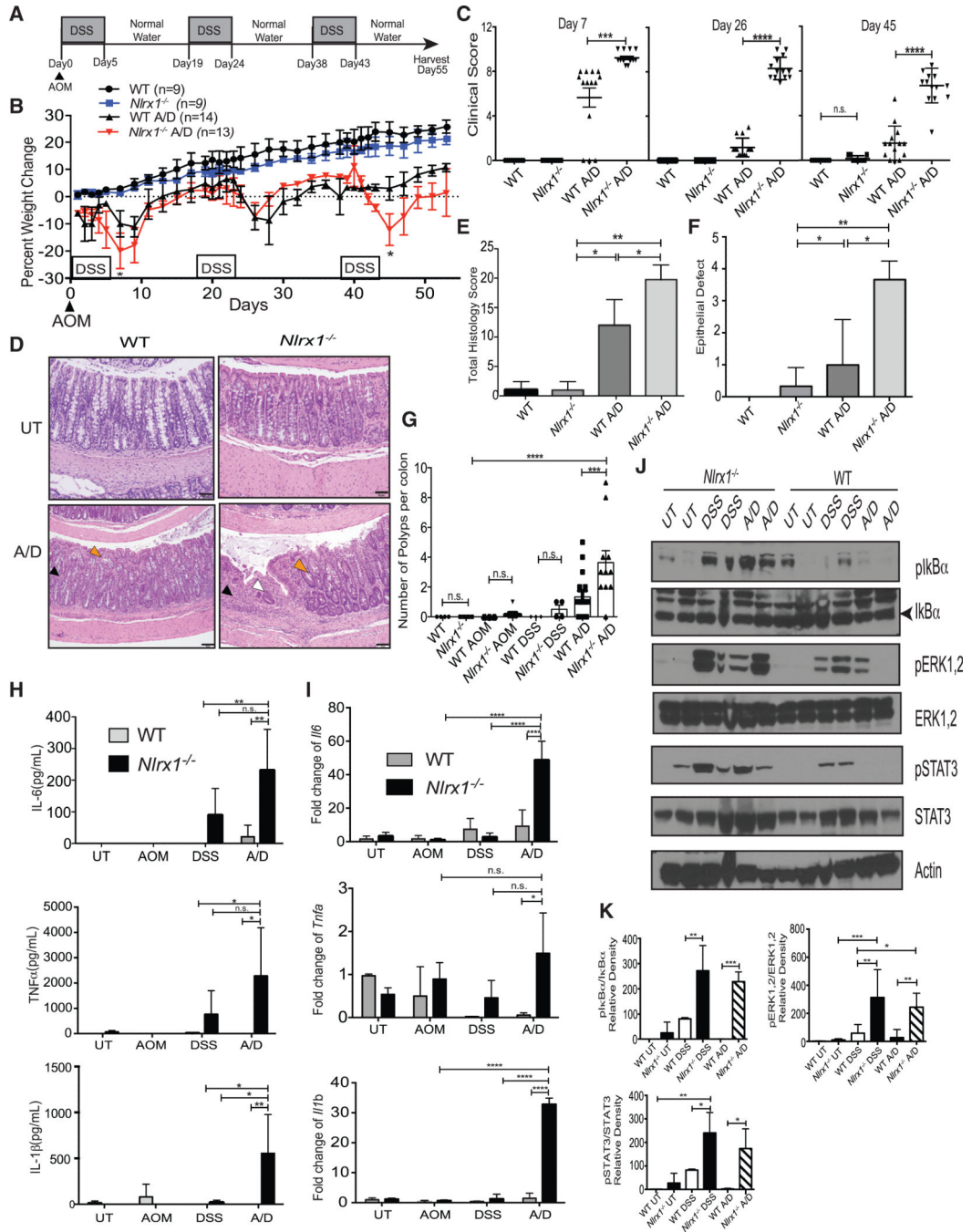


Figure 1. *Nlr1* Deficiency Leads to Increased Inflammation and Colitis-Associated Tumorigenesis

(A) In the chronic CAC model, WT and *Nlr1*^{-/-} mice were challenged with A/D.

(B) The percent weight change after A/D treatment is shown. Each data point is the average from three independent experiments with n indicated.

(C) Cumulative clinical scores were measured at days 7, 26, and 45. Each data point represents one animal.

(D) Photomicrographs show H&E-stained colons from untreated (UT) WT, UT *Nlr1*^{-/-}, A/D-treated WT with mild inflammation (black arrowhead) and crypt shortening (white

arrowhead), and A/D-treated *Nlrp1^{-/-}* with extensive inflammation (black arrowhead), crypt loss and atrophy (white arrowhead) and early mucosal dysplasia (orange arrowhead). Scale bars represent 50 μ m.

(E) Total histology score for UT or A/D-treated WT and *Nlrp1^{-/-}* mice scored in a blinded fashion.

(F) Average epithelial defects were measured from H&E stained colons as indicated. Graph is a compilation of three separate experiments.

(G) Quantification of macroscopic polyp formation in the colons of WT and *Nlrp1^{-/-}* mice after A/D treatment. Each data point represents one animal. Graph is a compilation of three separate experiments.

(H) Serum cytokine levels of IL-6, TNF- α , and IL-1 β were measured by ELISA. Values are averages from two independent experiments. n = 6 mice/group.

(I) Expression of *Il6*, *Tnf α* , and *Il1 β* transcript in colon homogenates was measured by qPCR using comparative C_T method (2^{-C_T}) and graphed as fold over UT WT sample (mean \pm SEM).

(J) Proteins isolated from distal colonic tissue obtained from UT or A/D-treated WT and *Nlrp1^{-/-}* mice were analyzed for NF- κ B, MAPK, and STAT3 activity by western blot analysis with indicated protein loading control. Each lane represents one animal.

(K) Densitometric measurement of western blots was obtained from three independent experiments. n = 5 mice/group, n.s., non-significant. *p < 0.05, **p < 0.01, ***p < 0.001, and ****p < 0.0001.

See also Figure S1.

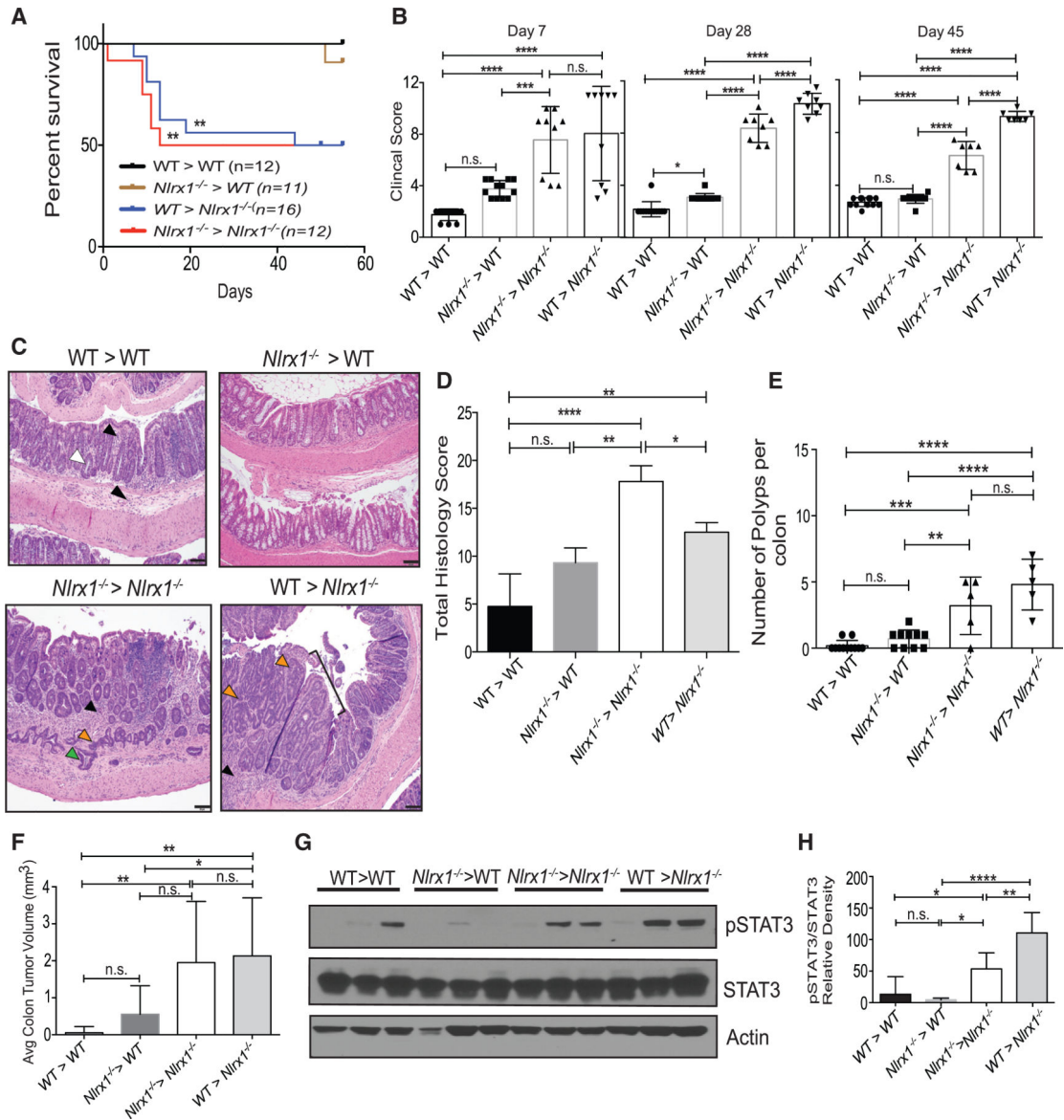


Figure 2. *Nlr1* Expression in the Non-hematopoietic Compartment Is Primarily Required for Protection against AOM/DSS-Induced Tumorigenesis

Bone-marrow chimeras of WT and *Nlr1*^{-/-} mice were challenged with AOM and 2.5% DSS (A/D).

(A and B) Mice from two independent experiments were monitored for (A) mortality and (B) clinical score of disease; n = 6 mice/group.

(C) Photomicrographs of H&E-stained colons from A/D-treated WT > WT with mucosal and submucosal inflammation (black arrowheads) and crypt shortening (white arrowhead); A/D-treated *Nlr1*^{-/-} > WT mice with similar features; A/D-treated *Nlr1*^{-/-} > *Nlr1*^{-/-} mice with extensive inflammation separating crypts (black arrowhead), crypt dysplasia (orange arrowhead), and partial penetration of muscularis mucosa (green arrowheads); A/D-treated WT > *Nlr1*^{-/-} mice with inflammation (black arrowhead) and a sessile adenoma

(bracket) with dysplasia, including crypt infolding and branching and loss of goblet cells and nuclear polarization (orange arrowheads). Scale bars represent 50 μm .

(D) Total histology score of colons represented in (C).

(E) Macroscopic colonic polyps were counted on day 55 post-A/D treatment. Each data point represents one animal. Graph is the compilation of two independent experiments.

(F) Average colon tumor volume was measured. n = 6 mice/group.

(G) Proteins isolated from distal portion of colons were analyzed by western blot for STAT3 activation. Each lane represents one animal.

(H) Densitometric measurement of western blots was obtained from three independent experiments. n = 5 mice/group, n.s., non-significant. *p < 0.05, **p < 0.01, ***p < 0.001, and ****p < 0.0001.

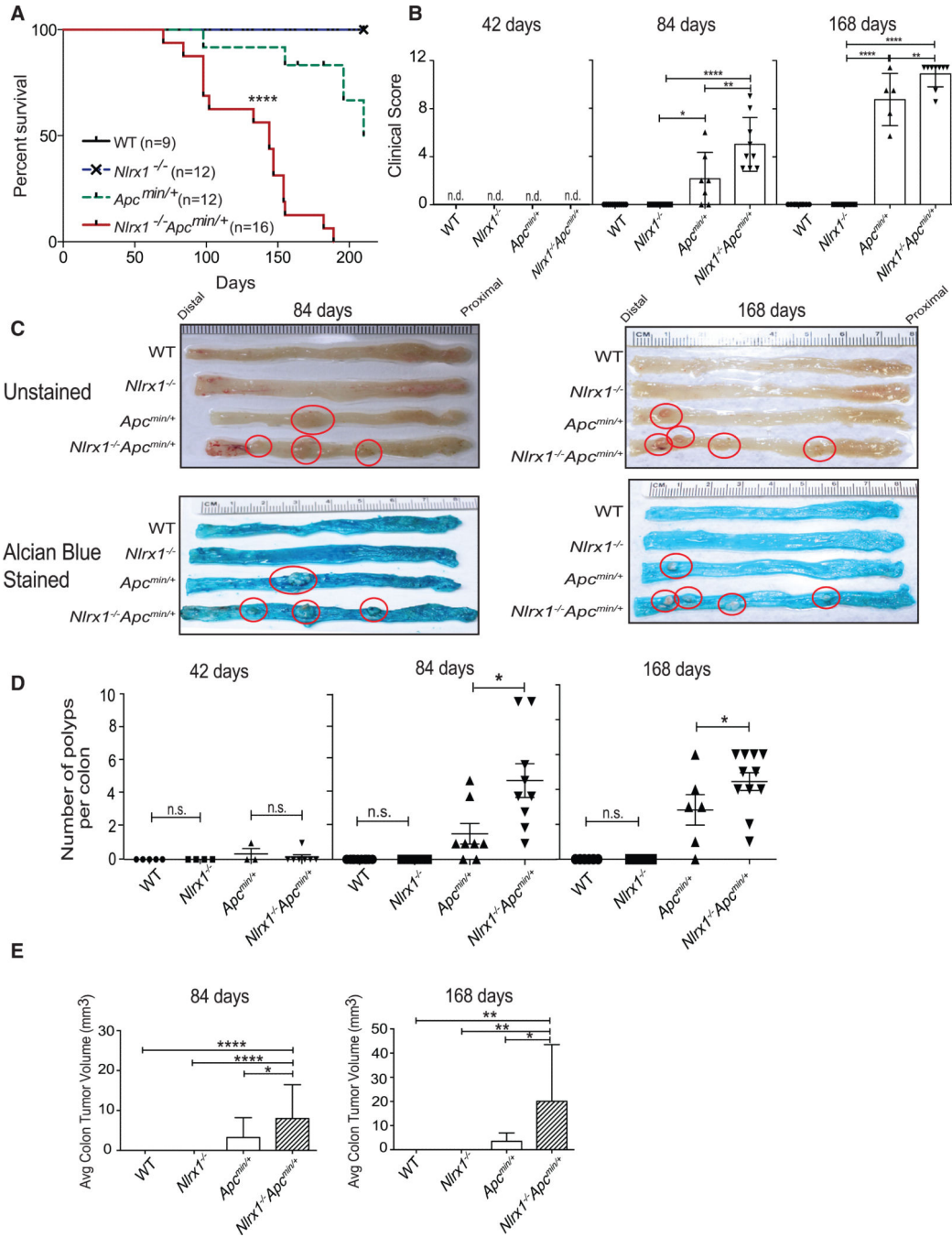


Figure 3. *Nlr1* Deficiency Leads to Increased Disease and Polyp Burden in the *Apc*^{min/+} Model and Sporadic CRC

(A) WT, *Nlr1*^{-/-}, *Apc*^{min/+}, and *Nlr1*^{-/-}*Apc*^{min/+} mice were followed for 168 days for long-term survival; n = 9 mice/group.

(B) Cumulative clinical score of WT, *Nlr1*^{-/-}, *Apc*^{min/+}, and *Nlr1*^{-/-}*Apc*^{min/+} mice at 42, 84, and 168 days. Images of WT, *Nlr1*^{-/-}, *Apc*^{min/+}, and *Nlr1*^{-/-}*Apc*^{min/+} mice at 84 and 168 days of age.

(C) Polyps in representative colons from mice at 84 (left) and 168 days (right) of age that were either unstained (top) or stained with Alcian blue. Polyps are highlighted by red circles.

(D and E) Quantification of macroscopic polyp formation and average tumor volume in the colons of WT, *Nlr1l*^{-/-}, *Apc*^{min/+}, and *Nlr1l*^{-/-}*Apc*^{min/+} mice at 42, 84, and 168 days of age. Each data point represents one animal. n = 5 mice/group, n.s., non-significant. *p < 0.05, **p < 0.01, and ****p < 0.0001.

See also Figure S2.

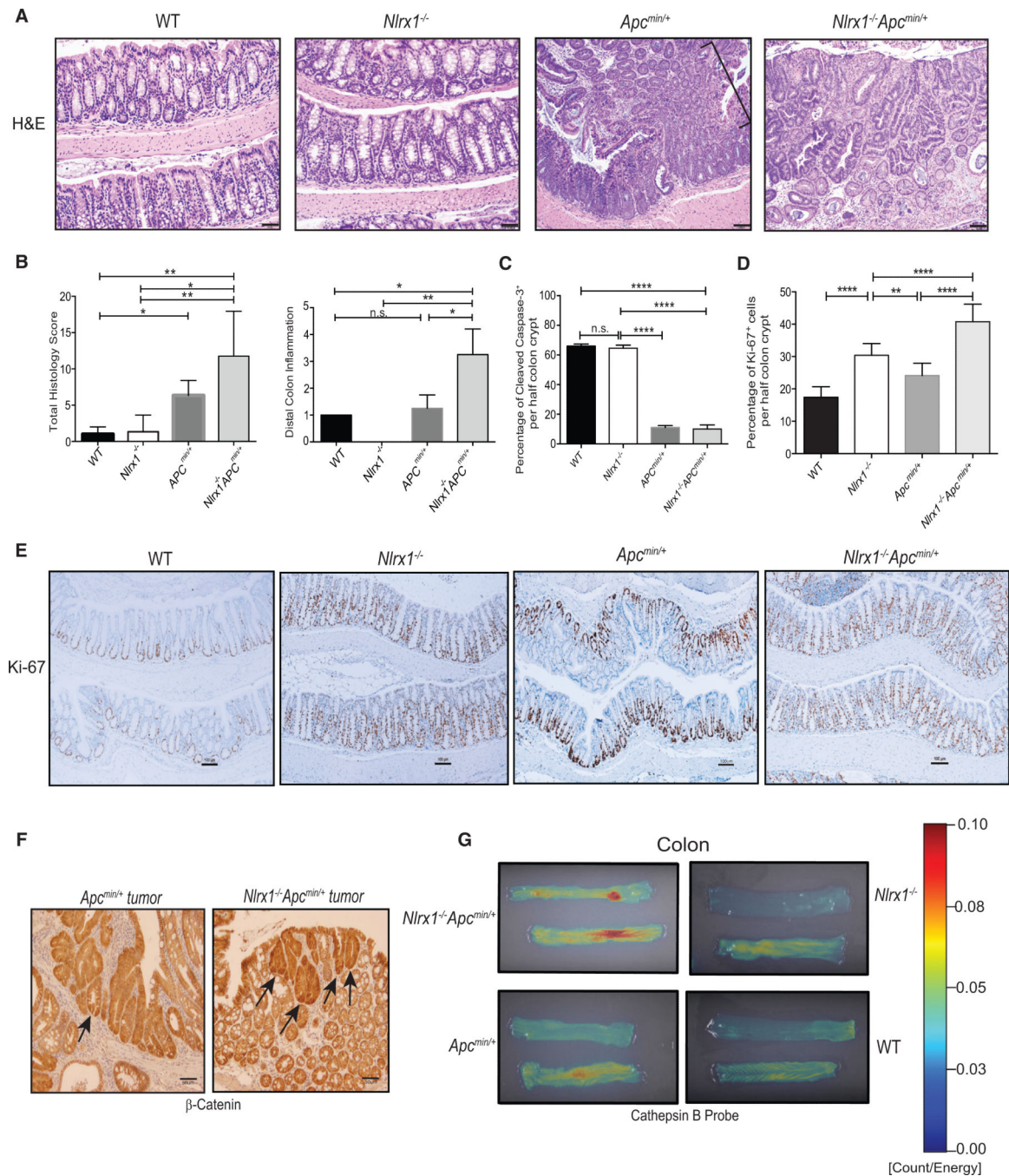


Figure 4. *Nlr1* Deficiency on the *Apc*^{min/+} Background Leads to Increased Proliferation and Greater Expression of the Tumor Biomarkers β -Catenin and Cathepsin B

(A) Photomicrographs of H&E-stained colons from WT, *Nlr1*^{-/-}, *Apc*^{min/+} mice displayed a pedunculated adenoma (bracket) with mucosal dysplasia, and *Nlr1*^{-/-}*Apc*^{min/+} colons depicted an area of mucosal dysplasia within an adenoma. Scale bars represent 50 μ m.

(B) Total Histology score and distal colon inflammation were determined in H&E-stained colon sections represented in A. All slides were scored in a blinded fashion.

(C–E) Quantification of positive cleaved caspase-3 (C) or Ki-67 (D) cells stained per half-length of crypt was determined from age-matched *Apc*^{min/+} and *Nlr1*^{-/-}*Apc*^{min/+} mice at

168 days of age shown in (E) for Ki-67. n = 4 mice/group, n.s., non-significant. *p < 0.05, **p < 0.01, ***p < 0.001, and ****p < 0.0001. Scale bars represent 100 μ m.

(F) Representative histological micrographs of *Apc^{min/+}* and *Nlr1^{-/-}Apc^{min/+}* colon tumors at 168 days stained with β -catenin are shown (arrows), n = 3 mice/group. Scale bars represent 50 μ m.

(G) Representative images of colons from WT, *Nlr1^{-/-}*, *Apc^{min/+}*, and *Nlr1^{-/-}Apc^{min/+}* mice at 168 days of age are shown. Fluorescent signals (with intensity scale shown to right) due to active cathepsin B cleavage of target probe were visualized by fluorescence reflectance imaging. n = 2 mice/group.

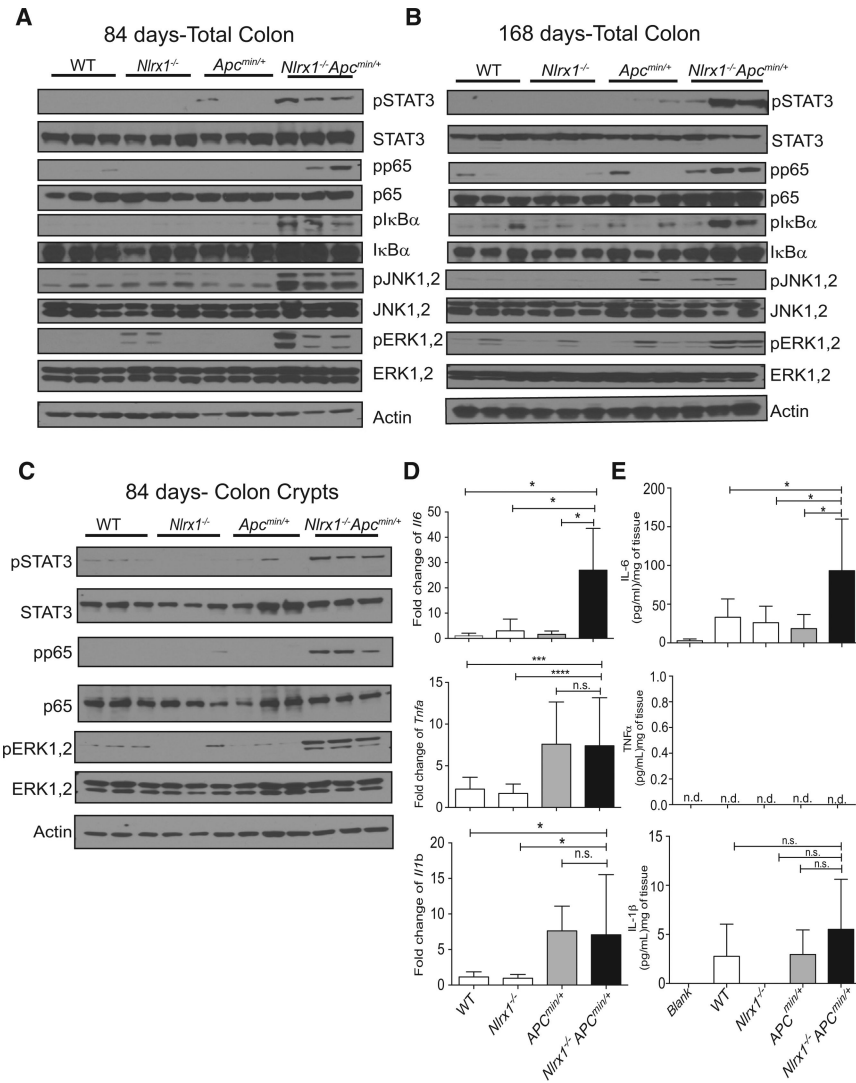


Figure 5. *Nlr1* Deficiency Contributes to Exacerbated NF- κ B, MAPK, and STAT3 Activation and IL-6 Production in the *Apc*^{min/+} Model

(A–C) Protein lysates were isolated from distal colon tissues obtained from WT, *Nlr1*^{−/−}, *Apc*^{min/+}, and *Nlr1*^{−/−}*Apc*^{min/+} mice at days 84 (A) and 168 (B), and isolated colon crypts from 84 days (C). Lysates were analyzed by western blot for NF- κ B, MAPK, and STAT3 activation. Each lane represents one animal; n = 3 mice/group.

(D) RNA was isolated from age-matched WT, *Nlr1*^{−/−}, *Apc*^{min/+}, and *Nlr1*^{−/−}*Apc*^{min/+} distal colonic tissues and analyzed by qPCR for expression levels of *Il6*, *Tnfa*, and *Ilb*, n = 3 mice/group.

(E) IL-6, TNF- α , and IL-1 β proteins produced by colon explants were analyzed by ELISA, n = 3 mice/group. n.s., non-significant. *p < 0.05, ***p < 0.001, and ****p < 0.0001.

See also Figure S3.

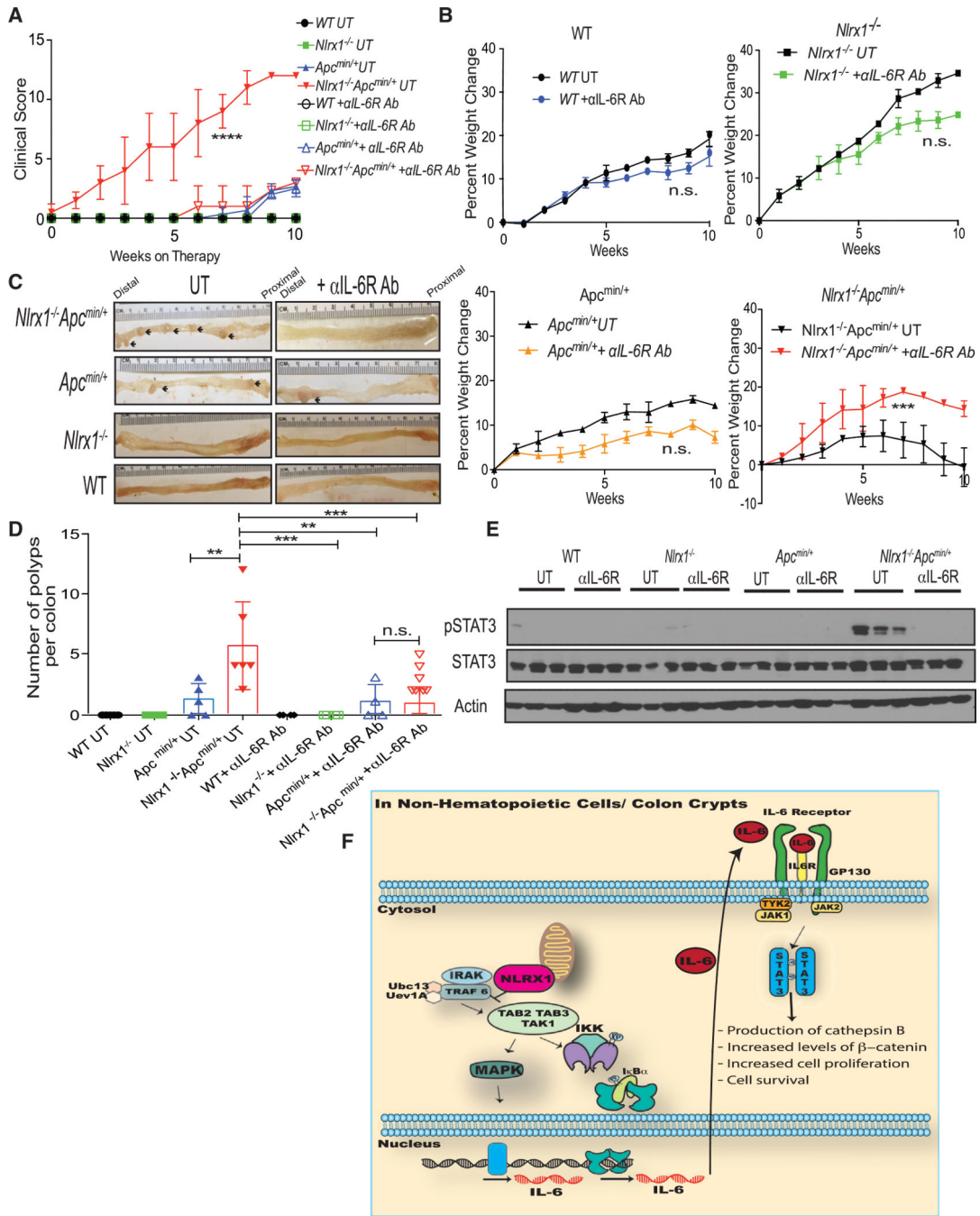


Figure 6. Inhibition of IL-6 Signaling in *Nlr1^{-/-}Apc^{min/+}* Mice Reduces Mortality and Tumorigenesis by Decreasing STAT3 Activation

(A) WT, *Nlr1^{-/-}*, *Apc^{min/+}*, and *Nlr1^{-/-}Apc^{min/+}* animals were subjected to anti-IL6R administration at 20 μg/ml/animal. Cumulative clinical score of animals on and off treatment were monitored.

(B) The percent weight change for animals that were untreated (UT) or given 10 weeks of anti-IL6R therapy is shown for each strain. n = 4 mice/group.

(C) Images are shown of colons isolated at 10 weeks after anti-IL6R therapy from WT, *Nlr1^{-/-}*, *Apc^{min/+}*, and *Nlr1^{-/-}Apc^{min/+}* animals with polyps indicated (arrows).

(D) Quantification of macroscopic polyp formation in the colons of UT or anti-IL6R-treated animals as indicated. Each data point represents one animal. n = 4 mice/group, n.s., non-significant. *p < 0.05 **p < 0.01, ***p < 0.001, and ****p < 0.0001.

(E) Protein lysates were isolated from distal colon tissues obtained from WT, *Nlr1^{-/-}*, *Apc^{min/+}*, and *Nlr1^{-/-}Apc^{min/+}* mice that were either left UT or were treated with anti-IL6R for 10 weeks. Lysates were analyzed by western blot for phosphorylated STAT3. Each band represents one animal; n = 3 mice/group.

(F) Model of NLRX1 negatively impacting NF- κ B and MAPK, which increase IL-6 to activate STAT3 and the downstream oncogenic cathepsin B and β -catenin pathways to increase proliferation in tumors.

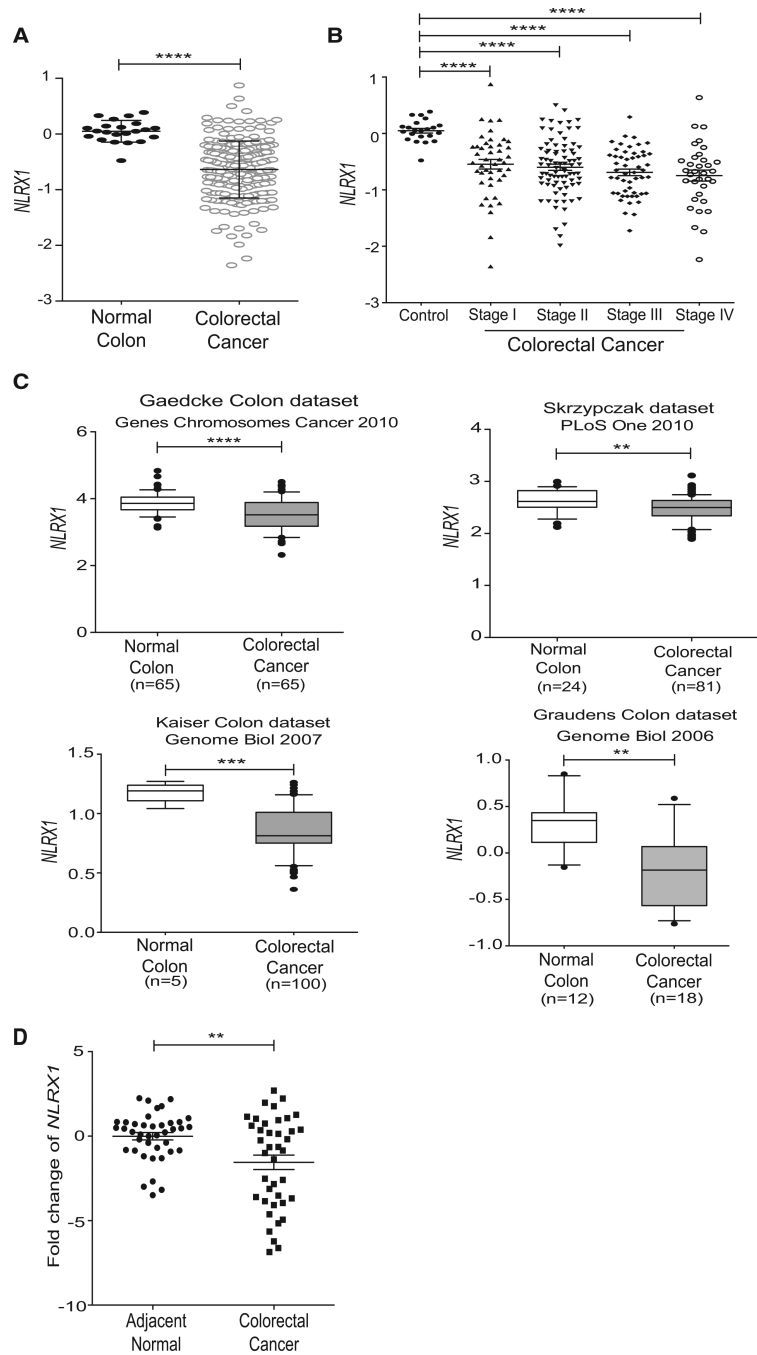


Figure 7. *NLRX1* Expression Is Reduced in Multiple Colorectal Cancer Patient Databases and in Clinical Samples

(A) CRC microarray databases were mined for *NLRX1* expression. The raw data were exported from the TCGA CRC database, with representations of 22 healthy control and 215 CRC samples. Mean \pm SEM, presented as Log₂ median-centered ratio expression. Unpaired Mann-Whitney test was used to evaluate the statistical significance.

(B) Correlation analysis compared expression levels of *NLRX1* among different stages of CRC progression. TNM stage information was exported from the TCGA colon database.

(C) Reduced *NLRX1* expression was found in four additional CRC databases. Log₂ median-centered ratio expression is presented for the four datasets used. Box plots were generated by GraphPad, whiskers are drawn down to the 10th percentile and up to the 90th percentile. Points below and above the whiskers are drawn as individual dots.

(D) *NLRX1* expression in human clinical CRC FFPE samples collected from a Chinese patient cohort (n = 40) was analyzed by qPCR using comparative C_T method (2^{-CT}) (mean ± SEM). **p < 0.01, ***p < 0.001, and ****p < 0.0001.